JOURNAL OF MATERIALS SCIENCE 33 (1998) 2679–2682

# Influence of buoyancy convection on solute distribution in Pd40Ni40P20 alloy

R. P. LIU*, J. H. ZHAO, X. Y. ZHANG, D. W. HE, L. L. SUN, Z. C. QIN, Y. F. XU, W. K. WANG
*Institute of Physics, Chinese Academy of Sciences, P.O. Box 603(34), Beijing 100080, People's Republic of China and *Institute of Materials Science and Engineering, Yanshan University, Qinhuangdao 066004, People's Republic of China*

The differences in the solute distribution in microstructure of Pd40Ni40P20 alloy solidified on board a Chinese retrievable satellite and on the ground were studied. In comparison with those crystallized under normal gravity conditions (1 ***g***), it was found that the P content was lower, but the Pd content was higher in the primary phase in microgravity conditions ($\mu$***g***). In the eutectic region the P content, however, was increased but the Pd content was decreased. The differences in solute distribution crystallized under 1 ***g*** and $\mu$***g*** conditions show the influence of buoyancy convection on the mass transport coefficient in liquids under normal gravity conditions. 

## 1. Introduction

Solidification processes of metals and alloys are affected by gravity-driven forces on earth, and it is difficult to eliminate them in ground-based experiments. The existence of buoyancy convection makes the analyses of solidification unclear in respect to mass transport by diffusion and convection. The space environment gives a new way to study solidification mainly dominated by pure diffusion [1, 2, 3]. This will undoubtedly lead to a better understanding of solidification.

Gravity effects on solute distribution were seldom considered in past studies of the solidification of alloys [4, 5, 6]. The subject of this paper was to study the differences in distribution of the alloying elements in the solid between the samples solidified both on board a Chinese recoverable satellite and on the ground. Additionally, some theoretical bases for space- and ground-based experiments in the future were provided.

## 2. Experimental procedure

Pd40Ni40P20 alloy ingots were prepared by arc melting the mixture of pure Pd (99.9 wt %) with $Ni_2P$, which was alloyed by sintering pure Ni (99.6%) with pure P (99.4 wt %). The analytic composition of the alloy was Pd40.6 at %, Ni40.0 at % and P19.4 at %. The container of the alloy was a dry and clean quartz ampoule with an inside Ta tube to prevent chemical reaction between the quartz tube wall and the $B_2O_3$ which was used as flux to avoid direct contact between the sample and the ampoule wall. Before sealing, the ampoule was evacuated to $2.7 \times 10^{-1}$ Pa.

One sample was solidified on board a Chinese retrievable satellite ($10^{-3} \sim 10^{-4}$ ***g***). After heating to 1173 K at a speed of 0.1 K $s^{-1}$ and being held for 150 min at this temperature, it was cooled at the rate of 0.056 K $s^{-1}$. The other reference samples were solidified on the ground (1 ***g***) at the cooling rates of 0.056 K $s^{-1}$, 0.11 K $s^{-1}$, and 0.67 K $s^{-1}$, respectively, with the same other experimental parameters as in the $\mu$***g*** experiment.

Microstructure and phase morphology were observed by optical microscopy (OM) and scanning electron microscopy (SEM). The solute distribution in microstructure was measured by energy dispersive X-ray spectroscopy (EDX). Phases were determined by X-ray diffractometry (XRD) and selected area electron diffractometry (SAED).

## 3. Results and discussion

The solidified microstructure was composed of primary phase (dendrites $Ni_5P_2$) and ternary eutectics ($PdNi + Pd_3P + Ni_5P_2$) in both cases. But the morphology, especially the primary phase morphology, was quite different, as shown in Fig. 1. In the microstructure solidified on the earth, the primary phase was coarse dendrites of $Ni_5P_2$. On the other hand, in the space sample, the primary dendrites of $Ni_5P_2$ were finer. The primary spacing values were 100 $\mu$m and 270 $\mu$m under $\mu$***g*** and 1 ***g*** conditions, respectively.

Although the microgravity environment did not change the type of phases, the solute distribution in microstructure was changed. EDX results for the solute distribution are shown in Table I. The Pd content was higher but the P content was lower in the primary phase under $\mu$***g*** conditions than those under 1 ***g*** conditions.

Theoretical researches [7, 8, 9] have already proved the existence of different solute distribution coefficient

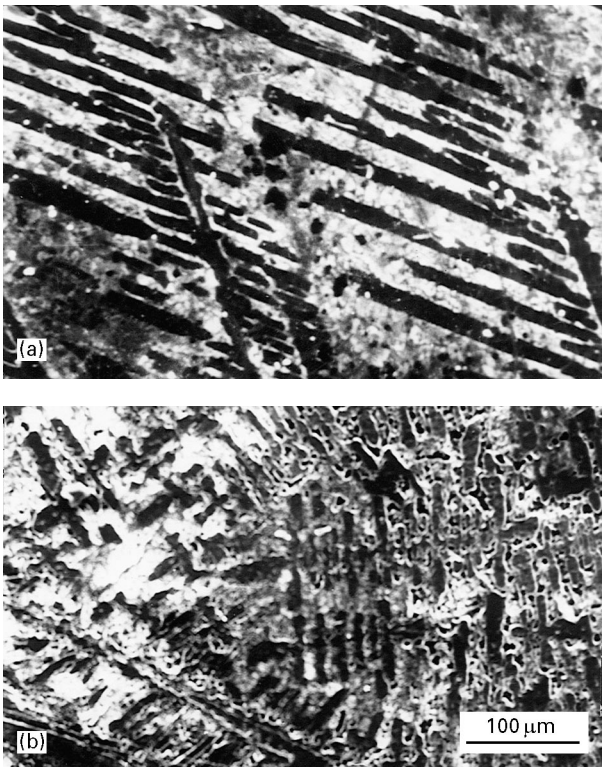


*Figure 1* Microstructure under 1 $g$ and μ$g$ conditions (a) 1 $g$, 0.056 K s$^{-1}$; (b) μ$g$, 0.056 K s$^{-1}$.

TABLE I Solute distribution in the microstructure

| Condition | μ$g$ | | 1 $g$ | |
|---|---|---|---|---|
| Structure | Primary | Eutectic | Primary | Eutectic |
| Pd | 29.32 | 58.93 | 22.81 | 54.84 |
| P | 21.63 | 17.46 | 26.57 | 16.89 |

values $K$ under μ$g$ and 1 $g$ conditions

$$K_{(\mu g)} = (K_0 + \beta + \beta_T)/(1 + \beta) \quad (1)$$

$$K_{(g)} = (K_0 + \beta + \beta_T - \beta_g)/(1 + \beta) \quad (2)$$

where $K_{(\mu g)}$ and $K_{(g)}$ are solute distribution coefficients under μ$g$ and 1 $g$ conditions, respectively. The dimensionless numbers $\beta$, $\beta_T$ and $\beta_g$ are

$$\beta = V/K_S \quad (3)$$

$$\beta_T = S_T D_L \Delta T/TK_S \quad (4)$$

$$\beta_g = B_i V_i \theta(\rho_i - \rho)\, \boldsymbol{g}/K_S \quad (5)$$

where $K_S$ is constant for chemical reaction; $S_T$ is soret number; $D_L$ is solute diffusion coefficient in liquid; $V$ is shifting velocity of the solid–liquid interface; $\Delta T$ is temperature gradient; $B_i$ is shifting ratio of the component atom; $V_i$ is volume of the component element; $\rho_i$ is density of the component element; $\rho$ is average density of the alloy; $\theta$ is position on the solid–liquid interface [$\theta = \cos(n, \boldsymbol{g})$]; $\boldsymbol{g}$ is gravity acceleration.

Compare Equation 1 with Equation 2

$$K_{\mu g} - K_{1g} = (K_0 + \beta + \beta_T)/(1 + \beta) - (K_0 + \beta + \beta_T - \beta_g)/(1 + \beta) = \beta_g/(1 + \beta)$$

Therefore

$$K_{\mu g} - K_{1g} = B_i V_i \theta(\rho_i - \rho)\boldsymbol{g}/K_S(1 + \beta) \quad (6)$$

It is clear from Equation 1 that gravity has no effect on the solute distribution coefficient under microgravity conditions. But under gravity conditions on the ground, the solute distribution will be unavoidably affected by gravity, as revealed in Equations 2 and 6. To a given alloy system, gravity effects will be related not only with the position at the interface ($\theta$) but also with the density difference ($\rho_i - \rho$), according to Equation 6. If the density of an element being considered is approximately equal to the average density of the alloy, i.e. ($\rho_i - \rho$) $\approx 0$ or $\beta_g \approx 0$, gravity will have no effects on the solute distribution coefficient. If the element density is evidently different from the average density of the alloy, $K$ will be a function of $\theta$ in addition to ($\rho_i - \rho$), as shown in Fig. 2. To the condition of ($\rho_i - \rho$) $> 0$ at position $A$ ($\theta < 0$), it is easy to find that gravity will make $K$ increase (or $K_{\mu g} < K_{Alg}$); however at position $B$ ($\theta > 0$), gravity will make it decrease (or $K_{\mu g} > K_{B1g}$). When the experimental parameters are with the same values except $\theta$ during the solidification experiment there will be the result of $K_{Alg} > K_{Blg}$ in the ground-based experiments. On the other hand, to the alloy system with ($\rho_i - \rho$) $< 0$, a contrary result will be achieved, i.e. $K_{Alg} < K_{Blg}$ on the ground. Different values of $K$ will first cause different solute distribution and different constitutional undercooling in front of the interface, then they will affect the growth velocity of the cellular or dendritic tip, and finally they will further change the morphology of the growing crystal into an irregular shape. In fact, no such peculiar structure caused by gravity has ever been reported by any researchers. Just as reported by Wang and Li [7], gravity does not affect $K$ seriously enough to cause the formation of a peculiar phase morphology. So we can conclude that there is a different solute distribution at different places on the interface because of the influence of gravity on $K$, but it still does not elucidate why there were different solute contents in the microstructure under 1 $g$ and μ$g$ conditions.

The most important difference between solidification in microgravity and gravity conditions is whether there is buoyancy convection or not in the liquid. Different convection conditions will show different mass transport abilities, so it is more appropriate to elucidate solute distribution phenomenon by analysing the influence of the buoyancy convection on the mass transport abilities.

To elucidate the mass transport phenomenon, Frohberg [10], as well as Tensi [1] separated, on the basis of the measurement of the diffusion coefficient in space, the mass transport coefficient $D_L$ (or the so-called integral diffusion coefficient) into two major parts

$$D_L = D_L^a + D_{con} \quad (7)$$

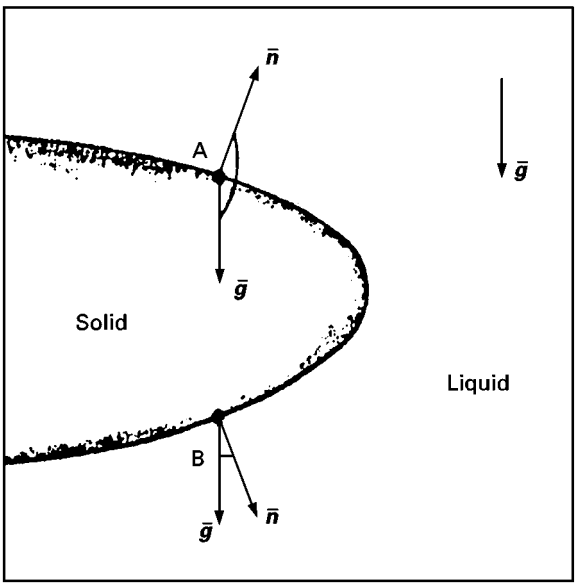


*Figure 2* Effect of position at the interface on solute distribution under gravity.

$D_L^a$ is the real atom diffusion coefficient; $D_{con}$ is the mass transport coefficient caused by convection.

In terms of Frohberg's separation of the mass transport coefficient, Tensi *et al.* [1] divided the mass transport coefficient under $1\,\boldsymbol{g}$ conditions ($D_{L1g}$) into two parts

$$D_{L1g} = D_{L\mu g} + D_{Lncon} \tag{8}$$

$D_{Lncon}$ is the mass transport coefficient caused by buoyancy convection; $D_{L\mu g}$ is the integral mass transport coefficient under $\mu\boldsymbol{g}$ conditions.

This formal separation of the integral diffusion coefficient in the liquid enables us to analyse the influence of buoyancy convection on the mass transport.

Combining Hunt's equation of primary spacing ($L$) for dendrites with this separation of $D_{L1g}$, we can evaluate the influence of buoyancy convection on mass transport.

According to Hunt's equation [5]

$$L = -\frac{64QmD_L(1-K_0)C_\infty}{R^{1/4}G^{1/2}} \tag{9}$$

Under $\mu\boldsymbol{g}$ and $1\,\boldsymbol{g}$ conditions,

$$L_{1g} = -\frac{64QmD_{L1g}(1-K_0)C_\infty}{R_{1g}^{1/4}G_{1g}^{1/2}} \tag{10}$$

$$L_{\mu g} = -\frac{64QmD_{L\mu g}(1-K_0)C_\infty}{R_{\mu g}^{1/4}G_{\mu g}^{1/2}} \tag{11}$$

so

$$\frac{L_{1g}}{L_{\mu g}} = \frac{D_{L1g}}{R_{1g}^{1/4}G_{1g}^{1/2}} \times \frac{R_{\mu g}^{1/4}G_{\mu g}^{1/2}}{D_{L\mu g}} \tag{12}$$

where $m$ is the slope of the liquid line; $Q$ is a constant caused by curvature undercooling; $K_0$ is the equilibrium solute distribution coefficient; $C_\infty$ is the solute concentration in the liquid far from the interface; $L_{1g}$, $L_{\mu g}$ are the primary spacing values under $1\,\boldsymbol{g}$ and $\mu\boldsymbol{g}$ conditions, respectively; $D_{L\mu g}$, $D_{L1g}$ are the integral mass transport coefficients in the liquid in front of the $S$–$L$ interface under $\mu\boldsymbol{g}$ and $1\boldsymbol{g}$ conditions, respectively; $R_{\mu g}$, $R_{1g}$ are the growth velocities under $\mu\boldsymbol{g}$ and $1\,\boldsymbol{g}$ conditions, respectively.

$$R = v/G \tag{13}$$

where $v$ is the cooling rate; $G_{\mu g}$, $G_{1g}$ are the temperature gradients in the liquid in front of the $S$–$L$ interface under $\mu\boldsymbol{g}$ and $1\,\boldsymbol{g}$ conditions, respectively.

For a small alloy ball (for example about 3 mm in diameter)

$$G_{\mu g} \approx G_{1g} \tag{14}$$

From Equations 12, 13 and 14

$$\frac{L_{1g}}{L_{\mu g}} = \frac{D_{L1g}}{D_{L\mu g}} \times \frac{v_{\mu g}^{1/4}}{v_{1g}^{1/4}} \tag{15}$$

$$\frac{D_{L1g}}{D_{L\mu g}} = \frac{L_{1g}}{L_{\mu g}} \times \frac{v_{1g}^{1/4}}{v_{1g}^{1/4}} \tag{16}$$

When $v_{1g} = v_{\mu g} = 0.056\,\mathrm{K\,s^{-1}}$

$$\frac{D_{L1g}}{D_{L\mu g}} = \frac{L_{1g}}{L_{L\mu g}} = \frac{270}{100} = 2.7$$

$$\frac{D_{L1g} - D_{L\mu g}}{D_{L\mu g}} = 170\%$$

Or according to Equation 8

$$\frac{D_{ln\,con}}{D_{L\mu g}} = 1.7$$

The mass transport coefficient under normal gravity conditions was 2.7 times as high as or 170% greater than that under microgravity conditions at the cooling rate of $0.056\,\mathrm{K\,s^{-1}}$ for Pd40Ni40P20 alloy. Or, the mass transport coefficient under buoyancy convection was 1.7 times as high as the integral mass transport coefficient in space. This means, under $1\,\boldsymbol{g}$ conditions, that the mass was mainly transported by buoyancy convection in the liquid in front of the $S$–$L$ interface, or mass transport caused by buoyancy convection played a dominant role under the $1\,\boldsymbol{g}$ condition.

When $L_{1g} = L_{\mu g} = 100\,\mu\mathrm{m}$ at $v_{1g} = 0.67\,\mathrm{K\,s^{-1}}$ and $v_{\mu g} = 0.056\,\mathrm{K\,s^{-1}}$ under $1\,\boldsymbol{g}$ and $\mu\boldsymbol{g}$ conditions, respectively

$$\frac{D_{L1g}}{D_{L\mu g}} = \frac{v_{1g}^{1/4}}{v_{\mu g}^{1/4}} = \frac{0.67^{1/4}}{0.056^{1/4}} = 1.86$$

Therefore

$$\frac{D_{L1g} - D_{L\mu g}}{D_{L\mu g}} = 86\%$$

Therefore

$$\frac{D_{ln\,con}}{D_{L\mu g}} = 0.86$$

The mass transport coefficient under $1\,\boldsymbol{g}$ conditions was 1.86 times as great as or 86% higher than that under $\mu\boldsymbol{g}$ conditions, or the mass transport coefficient under buoyancy convection was still 86% as high as the integral mass transport coefficient in space when the same primary spacing values were obtained at the cooling rates of $0.056\,\mathrm{K\,s^{-1}}$ in space and $0.67\,\mathrm{K\,s^{-1}}$

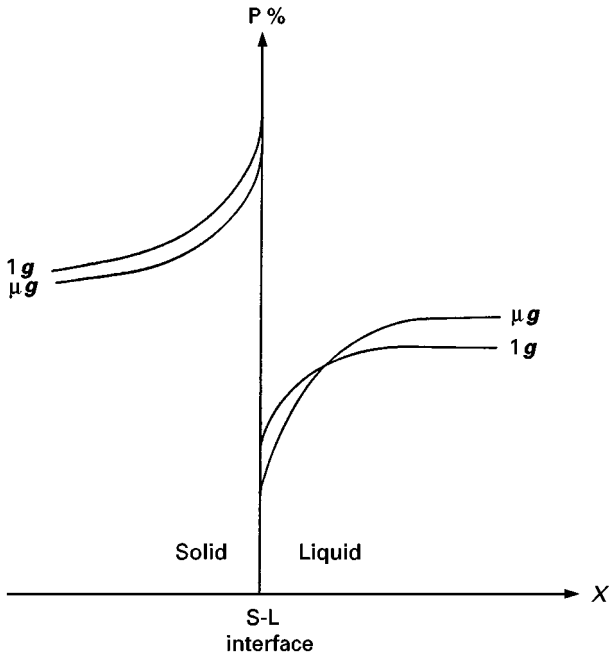


*Figure 3* Diagrammatic illustration of phosphorus distribution near the interface.

on the Earth, respectively. In other words, the contribution of buoyancy convection to the mass transport still played an important role during the solidification process on the ground.

To confirm the reliability of this evaluation, several other workers' reports on measurement of the diffusion coefficient in space can be reviewed. Frohberg *et al.* [10] tested the integral self-diffusion coefficient of Sn, which was 10–50% higher in the bulk liquid under $1\,\boldsymbol{g}$ conditions than that under $\mu\boldsymbol{g}$ conditions; Tensi *et al.* [12] estimated the integral diffusion coefficient of Cu in AlCu0.3 alloy, which was about 30% higher in bulk liquid, but almost seven times higher near the interface under $1\,\boldsymbol{g}$ conditions than those under space conditions. Our theoretical evaluation of the mass transport coefficients on the basis of experimental measurements of dendritic spacing is reliable in comparison with their reports.

The difference in solute distribution shown in the microstructure can be easily explained by the above discussion on the integral mass transport coefficient. According to the binary equilibrium phase diagram, $K_0 \approx 0$ for phosphorus. The phosphorus atoms would therefore be concentrated in the solid side near the interface. The more homogeneous is the liquid, the nearer is the solidification to the equilibrium condition, and so the higher is the content of phosphorus in the primary phase. Buoyancy convection under $1\,\boldsymbol{g}$ conditions made the liquid more homogeneous in composition and the final phosphorus content in the primary phase was higher than that under $\mu\boldsymbol{g}$ conditions. Fig. 3 is the diagrammatic illustration of the phosphorus distribution near the interface. On the other hand, for Pd, because the primary phase was phosphide of Ni with a small amount of Pd atoms dissolved in the lattice, the average Pd content (40 at %) was too high to dissolve in the lattice [13]. This was similar to the condition of $K_0 < 1$, and the influence of buoyancy convection on the Pd content in the primary phase was just the opposite to that of P. So, the Pd in the primary phase under $1\,\boldsymbol{g}$ conditions was lower than that under $\mu\boldsymbol{g}$ conditions.

## 4. Conclusions

The mass transport coefficient $D_{\text{Incon}}$ under $1\,\boldsymbol{g}$ conditions was 1.7 times as large as the integral mass transport coefficient under $\mu\boldsymbol{g}$ conditions, with the primary spacing of dendrites being 100 μm under $\mu\boldsymbol{g}$ and 270 μm under $1\,\boldsymbol{g}$ at the cooling rate of $0.056\,\text{K}\,\text{s}^{-1}$. But even when the same primary spacing values 100 μm were obtained, $D_{\text{Incon}}$ in front of the interface under $1\,\boldsymbol{g}$ was still 0.86 times as great as the integral mass transport coefficient under $\mu\boldsymbol{g}$. This was considered as the contribution of buoyancy convection.

Solute distribution in the microstructure was different in both conditions. The P content was lower, but the Pd content was higher in the primary phase crystallized under microgravity conditions than under gravity conditions. This was caused by two mechanisms: the difference in the binary distribution coefficients for P in Ni ($K_0 \approx 0$) and Pd in Ni ($K_0 < 1$) and the additional buoyancy convection under $1\,\boldsymbol{g}$ conditions. Buoyancy convection should not be neglected in investigations of solidification in ground-based experiments.

## References

1. H. M. TENSI and R. RÖSCH, in Proceedings of the Norderney Symposium on Scientific Results of the German Spacelab Mission D-2 (1995) p. 395.
2. H. NGUYEN THI, Q. LI, B. BILLIA, D. CARNEL, B. DREVET and J. J. FAVIER, in Proceedings of the Norderney Symposium on Scientific Results of the German Spacelab Mission D-2 (1995) p. 379.
3. M. STEHLE and S. REX, in Proceedings of the Norderney Symposium on Scientific Results of the German Spacelab Mission D-2 (1995) p. 387.
4. R. F. WOOD, *Phys. Rev. B* **25** (1982) 2786.
5. M. J. AZIZ, *Mater. Sci. Eng.* **93** (1988) 369.
6. H. Q. HU, "Metal Solidification" (Metallurgical Industry Press, Beijing, 1985).
7. S. Q. WANG and Q. C. LI, in Proceedings of the Symposium on the National Microgravity Science and Application Conference, Suzhou, 1991.
8. B. FEUERBACHER, "Materials Science in Space", edited by B. Feuerbacher (Springer Verlag, Berlin, 1986) p. 56.
9. U. MALMEJAC and J. P. PRAIZEY, in Proceedings of the 5th European Symposium: Mater Sci, Paris, 1984.
10. G. FROHBERG, in "Materials Science in Space" (Springer Verlag, Berlin, 1986) p. 118.
11. J. D. HUNT and C. MACKRODT, *Solidification and Casting of Metals*: proceedings of an international conference on solidification (1977) 3.
12. H. M. TENSI, *Metallkde* **81** (1990) 367.
13. E. WACHTEL, *ibid.* **76** (1985) 120.

*Received 15 November 1996*
*and accepted 5 February 1998*